On The Influence of Physical Processes on the Transient Pyrolysis of Cellulosic Samples

COLOMBA DI BLASI
Dipartimento di Ingegneria Chimica, Universitá degli Studi di Napoli Federico II
Piazzale V. Tecchio, 80125 NAPOLI, Italy

ABSTRACT

A two-dimensional, variable property, mathematical model of the transient pyrolysis of dry cellulosic materials, in response to prescribed conditions in a furnace, is presented. Chemical processes account for a reduction in the degree of polymerization of the solid and two competing pathways leading, respectively, to a solid charred residual (char) and low molecular weight gaseous species (gas) and to condensable organic components (tar). Volatile pyrolysis products flow towards both the cold solid and the hot char, with pressure and velocity variations described according to the Darcy law. Radiative, convective and conductive heat transfer interior to the solid and convective and radiative heat losses from the surfaces are also modeled. The pyrolysis of large samples is a wave-like process, controlled by heat transfer for a wide range of heating conditions (furnace temperatures from 600K to 1200K) and affected by the grain structure of the solid. Volatile pyrolysis products flow mainly along the solid grain, carrying thermal energy out from the sample. The total heat transferred to the solid is initially larger along this direction, because of the larger thermal conductivities. However, for long times, the total heat convected out almost equals the total heat conducted in. Larger temperatures along the char layer and a faster advancement of the pyrolysis front are predicted for the cross grain direction. Most of the pyrolysis products are tars with increasing char yields as reaction temperatures are lowered through variations in the sample heating conditions.

Key words: cellulosic materials, anisotropy, pyrolysis, modeling.

INTRODUCTION

The burning behavior of solid materials is characterized by two main parts [1]: the solid phase problem (distribution of composition and rate of generation of fuel vapors from the degrading solid) and the gas phase problem (oxidation of the devolatilization products with flaming combustion). In this study the solid phase problem is theoretically treated for a complex porous solid, such as wood, that is, for conditions where solid thermal degradation plays a key role in the fire growth.

The mathematical description of wood pyrolysis is very complex not only because chemical processes are made by a series of reactions involving hundreds of chemical species and strongly interact with transport phenomena, but also because only limited information is available on the kinetic mechanisms and data, and variation of physical properties. Recently, in view of utilizing wood and other cellulosic materials as

renewable sources of energy, some models [2-4] have been proposed where multi-step kinetic schemes have been coupled to the description of main physical processes. These models and the simpler one-step reaction models applied to the study of flammability characteristics of cellulosic materials have been recently reviewed [5] and will not be considered further here. However, it should be pointed out that experimental evidence has shown that many of the assumptions usually made are not always justified: the one-step global pyrolysis model cannot account for the competition [6,7] between char and volatile formation and physical processes are much more complex than the simple heat conduction equation frequently employed. Furthermore, all the theoretical analyses of wood pyrolysis are based on one-dimensional models which cannot adequately describe the anisotropic structure of the material and its implications in the thermal conversion process.

This study presents a two-dimensional unsteady mathematical model providing a quantitative representation of most of the interacting processes taking place during pyrolysis of cellulosic materials. The aim of the study is to clarify the interaction between chemistry and physics of the solid phase to improve the understanding of fire behavior.

MATHEMATICAL FORMULATION OF THE PROBLEM

To describe the competing primary reactions of wood pyrolysis, semi-global models [5], based on the lumping of the different products into three groups: char (the solid residual), gas (low molecular weight gaseous species: mainly CO, CO_2, H_2 and $C_1 - C_2$ hydrocarbons), and tar (all condensable, high molecular weight, organic components), can be used. However, reliable kinetic data for such mechanisms applied to wood degradation are not available [5]. Therefore, in this study a well known mechanism of cellulose pyrolysis [6,7] is used to model primary degradation of the solid:

$$SOLID \xrightarrow{k_1} ACTIVE\ SOLID \begin{cases} \xrightarrow{k_3} TAR \\ \xrightarrow{k_2} CHAR + GAS \end{cases}$$

This approach seems applicable because cellulose and hemicellulose account for about 75% of wood composition (cellulose (c. 50%), hemicellulose (c. 25%), the remaining part being lignin) and, even though these components exhibit different thermal stability

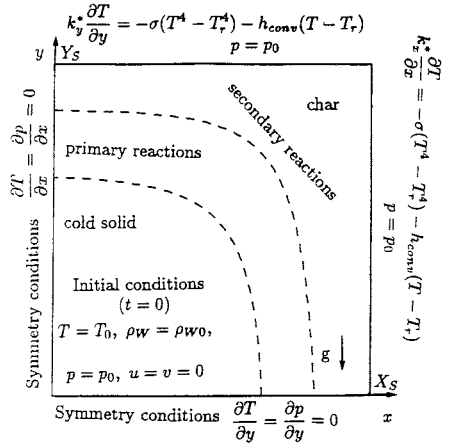

Figure 1 - Schematic of the solid degradation problem.

characteristics, some similarity exists between their kinetics of degradation. Secondary reactions of primary pyrolysis products and gasification of char are not taken into account at this stage.

From the physical point of view, the model here presented describes the transport phenomena occurring through the cross section of a wooden sample exposed in a pre-heated, inert atmosphere furnace. Wood is an anisotropic material with different properties along, cross and tangential to the grain [8]. Thermal conductivity across and tangential to the grain direction is approximately one third that along the grain [8]. Also, the permeability to gas flow across the wood grain is much lower than that along the other two directions [8] (up to a factor of 10^4). To study the effects of wood anisotropy on the thermal degradation, different properties along the x and y directions are assigned. Because of the symmetry of the problem, only one fourth of the sample is considered, according to the schematic reported in Fig. 1 (initial and boundary conditions of the mathematical model are also included in this figure).

The formulation of the mathematical model is based on the assumptions of constant volume occupied by the cell wall sample as the solid undergoes pyrolysis (no thermal swelling and/ or shrinkage and surface regression), local thermal equilibrium between the solid matrix and the volatiles, and no condensation of tar if any migrates through the cold solid. The mathematical model, numerically solved [9], is made by the balance equations for solid phase species (eqns. (1-3), solid, active solid and char), gas phase species (total continuity eqn. (4)), energy (eqn.(5)), momentum (eqns.(6-7)), state equation and solid volume variation (eqns. (8-9)):

$$\frac{\partial \varrho_W}{\partial t} = -r_1, \quad \frac{\partial \varrho_A}{\partial t} = r_1 - r_2 - r_3, \quad \frac{\partial \varrho_C}{\partial t} = \nu_C r_2 \qquad (1-3)$$

$$\frac{\partial(\varepsilon \varrho_g)}{\partial t} + \frac{\partial(\varrho_g u)}{\partial x} + \frac{\partial(\varrho_g v)}{\partial y} = \nu_G r_2 + r_3 \qquad (4)$$

$$\frac{\partial}{\partial t}(\varrho_C h_C + \varrho_W h_W + \varrho_A h_A + \varepsilon \varrho_g h_g) + \frac{\partial}{\partial x}(\varrho_g h_g u) +$$

$$\frac{\partial}{\partial y}(\varrho_g h_g v) = \frac{\partial}{\partial x}\left(k_x^* \frac{\partial T}{\partial x}\right) + \frac{\partial}{\partial y}\left(k_y^* \frac{\partial T}{\partial y}\right) + \sum_{k=1,3} r_k \Delta h_k \qquad (5)$$

$$u = -\frac{K_x}{\mu}\frac{\partial p}{\partial x}, \quad v = -\frac{K_y}{\mu}\left(\frac{\partial p}{\partial y} + \varrho_g g\right) \qquad (6-7)$$

$$p = \frac{\varrho_g R T}{W_g}, \quad \frac{V_s}{V_{s0}} = \frac{(\varrho_W + \varrho_C + \varrho_A)}{\varrho_{W0}} \qquad (8-9)$$

where $K_k = A_k exp(-E_k/RT)$ $k = 1, 3$, $r_1 = A_k exp(-E_k/RT)\varrho_W$,
$r_k = A_k exp(-E_k/RT)\varrho_A$, $k = 2, 3$,
$\varrho_W = M_W/V$, $\varrho_C = M_C/V$, $\varrho_g = M_g/V_g = M_g/(\varepsilon V)$, $\varepsilon = V_g/V$, $V_g = V - V_s$,
$h_W = c_W(T - T_0)$, $h_C = c_C(T - T_0)$, $h_g = c_g(T - T_0)$,
$k_x^* = \eta k_{Wx} + (1-\eta)k_{Cx} + \varepsilon k_g + \sigma T^3 d_x/\omega$, $k_y^* = \eta k_{Wy} + (1-\eta)k_{Cy} + \varepsilon k_g + \sigma T^3 d_y/\omega$,
$K_x = \eta K_{Wx} + (1-\eta)K_{Cx}$, $K_y = \eta K_{Wy} + (1-\eta)K_{Cy}$, $\eta = (\varrho_A + \varrho_W)/\varrho_{W0}$.
The symbols have the following meaning: A pre-exponential factor, E activation energy, ϱ density, ν stoichiometric coefficient, ε porosity, u and v velocity components, Y mass fraction, T temperature, c thermal capacity, k thermal conductivity, D diffusion

coefficient, M mass, V volume, Δh heat of reaction, K permeability, μ viscosity, p pressure, W molecular weight, σ Stefan-Boltzman constant, ω emissivity, d pore diameter. Subscripts indicate: W cellulose, C char, A active cellulose, O oxygen, G gas, g total volatiles, 0 initial or reference conditions.

RESULTS

In this section some results of numerical simulations of the pyrolysis process are discussed. The kinetic data are taken from [7], whereas the values of the heat of pyrolysis are the same used in [4]. Medium properties describe wood and are again assigned as in [4]. Thermal conductivities are taken from [10] and permeabilities have been estimated to give gas overpressures of the same order of those experimentally observed [10]. Values along the x and y directions are chosen to describe cross (low values) and parallel (high values) grain properties: $k_{Wx} = k_{Ax} = 10.5 \times 10^{-2}$, $k_{Cx} = 7.1 \times 10^{-2}$, $k_{Wy} = k_{Ay} = 25.5 \times 10^{-2}$, $k_{Cy} = 10.46 \times 10^{-2} W/mK$; $K_{Wx} = K_{Ax} = 1 \times 10^{-5}$, $K_{Cx} = 5 \times 10^{-1}$ $K_{Wy} = K_{Ay} = 1 \times 10^{-1}$, $K_c = 5$ darcys. All simulations have been made for a sample size of $0.02m \times 0.02m$. The furnace temperature, T_r, is initially 500K and then it is increased, with a rate of $10K/s$, to a prescibed final value, T_f, varying from 600K to 1200K.

An example of the dynamics of the degradation process is presented for $T_f = 900K$. The reaction process is initially localized along the external boundary of the sample and, as time increases, it assumes a wave-like character. Formation of active cellulose starts at temperature values of about 550K. The propagation of this reaction front is followed by that of the charring reaction (2) and, with a slight delay, by that of tar formation (3). As can be observed from Fig. 2, where the contours of the rate of reaction (3) are reported for three successive times, the reaction front propagates, with decreasing rate, towards the center of the sample. The increasing distance from the exposed surfaces causes progressively lower maximum values of the reaction rate and a slight enlargment of the thickness of the reaction zone. The different properties used along the two directions lead to different rates of propagation. More precisely, as in the experiments [2,8,10], a faster advancement is predicted along the x direction (cross grain).

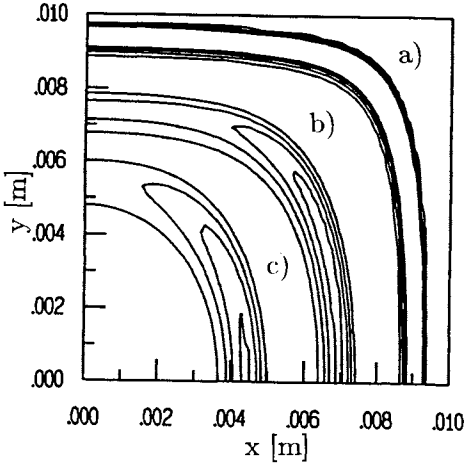

Figure 2 - Constant contour levels of the reaction rate of tar formation (3) for t=50s (a), 125s (b) and 200s (c) and $T_f = 900K$. Values $[kg/m^3 s]$ from 4 and with step 3.

The grain structure of the solid strongly affects the flow of volatile pyrolysis products through the pores. Figure 3 reports the pressure contours and the vector velocity field for four successive times. Thermal degradation is initially faster in the neighborhood of the right boundary, that is cross grain. Thus, for short times, a significant mass outflow is observed along this region. However, since the char permeability to gas flow is larger along grain, very high values of the mass efflux are also reached through a narrow region of the upper boundary, close to the vigorous pyrolysis zone. The formation of volatile products in a partially reacted medium (pyrolysis region), where porosity and permeability are still low, and the migration of volatile products towards the unreacted solid cause the pressure to increase across a rather wide zone, parallel to solid grain.

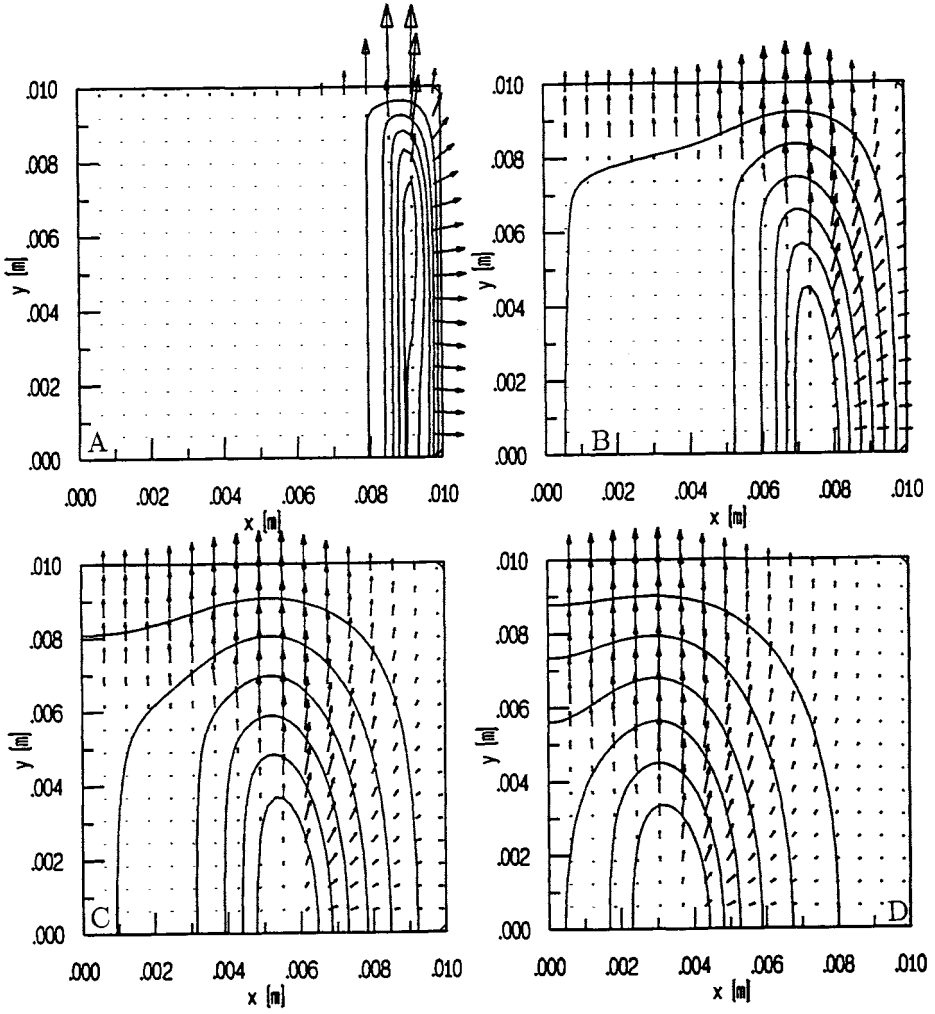

Figure 3 - Constant contour levels of gas overpressure [atm] from 1 and then with step 0.05 and vector velocity field for t=25s (A), 85s (B), 145s (C) and 205s (D) and $T_f = 900K$. Maximum vector velocity [m/s]: 0.22 (A), 0.11 (B), 0.09 (C) and 0.078 (D).

As time increases and significant degradation takes place also along the grain direction, volatile products flow mostly along this direction and escape from the upper boundary. In accordance with the wave-like character of the process, the gas overpressure front propagates towards the centerline of the sample and, similarly to the reaction fronts, slightly enlarges. The flow velocity, which is the result of the volatile release rate and pressure gradients, attains successively lower values as degradation proceeds, because of the continuosly decreasing reaction temperatures. The char region, perpendicular to solid grain, where very slow convection exists, also becomes larger. For very long times, no volatile flow is observed from the right boundary, while there is a tendency towards an increase of the mass escaping from the upper boundary, as a consequence of the enlargment of the reaction zone. Finally, very low velocities directed towards the cold solid are simulated.

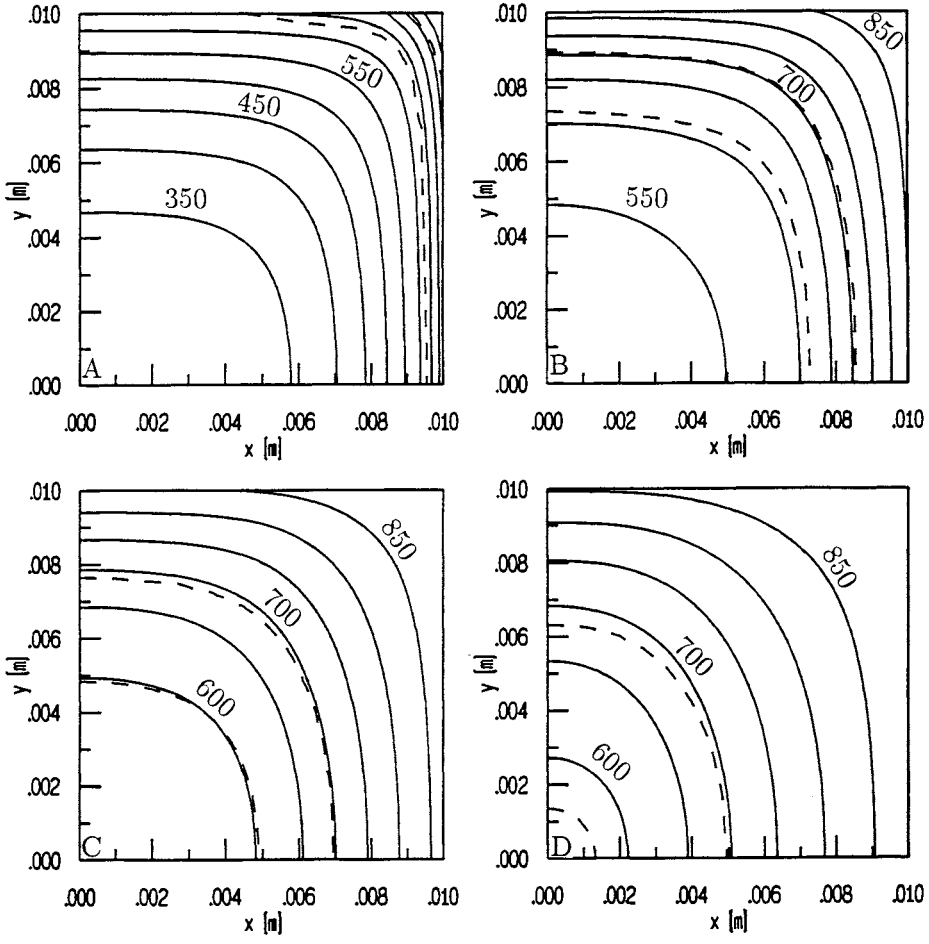

Figure 4 - Isotherms [K] (solid lines: values reported in the figure and step 50) and contours of the conversion factor η (dashed lines) equal to 0.01 and 0.99 for t=25s (A), 85s (B), 145s (C) and 205s (D) and $T_f = 900K$.

In general, the low flow of hot pyrolysis products pre-heats the virgin solid making the rate of primary pyrolysis faster. On the contrary, transport of hot volatile products towards the charred surface cools the pyrolysis region. The formation of a thick low thermal conductivity char layer also hinders heat conduction from the exposed surface to the interior of the solid. Given that the solid is porous, radiation may be another mode of heat transfer, mainly along the char and pyrolysis regions where rather high temperatures are reached. Some insight of the time and space evolution of the temperature field can be obtained from Fig. 4, where the isotherms for four successive times are shown and Fig. 5 giving the time history of temperature at selected points of the computational domain. Figure 4 also reports the contours of $\eta = (\varrho_A + \varrho_W)/\varrho_{W0}$ of values 0.01 and 0.99, delimiting the regions where charring and devolatilization reactions take place (pyrolysis region). A comparison of the temperature values along the two directions shows that, in agreement with experiments [2,8,10], a faster increase along the virgin solid is predicted for the grain direction, whereas the surface temperature rises more slowly. This is due to thermal conductivities of the virgin and activated solid being larger along the y direction. As a consequence of the larger temperatures, the devolatilization rate is initially faster for the cross grain direction. A change in the temperature trend, beyond the pyrolysis region, corresponding to a plateau in the (time) temperature profile, is predicted. Again, in agreement with experiments [8,10], large values are reached along the inert char layer for the cross grain direction (x) where also a faster advancement of the pyrolysis front is established. The explanation of such a behavior is complex because, at this stage, all contributions in the energy balance equation are different from zero. However, since lower values of both the char and solid thermal conductivities would make the conversion time longer, it can be inferred that the reduced convective transport plays a role of great importance for the enhanced reaction process across the solid grain (x).

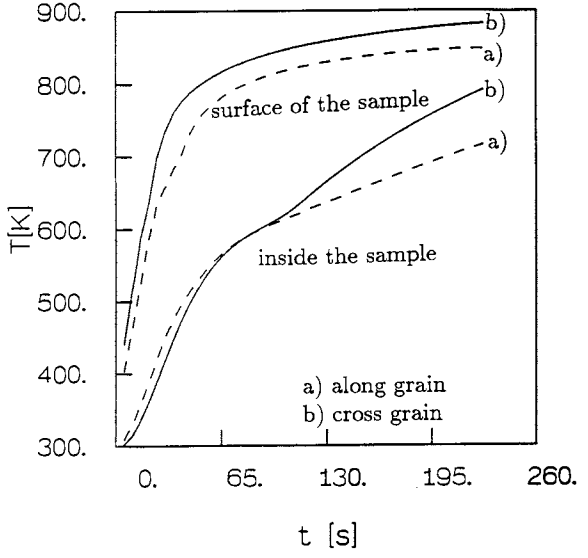

Figure 5 - Time history of temperature at the upper (a1: x=0 m, y=0.01 m) and right boundary (a2: x=0.01 m, y=0 m) and two selected positions along the x and y axes (b1: x=0 m, y=0.007 m; b2: x=0.007m, y=0 m) and for $T_f = 900K$.

In order to evaluate the role played by the different heat transfer mechanisms during the conversion process, the energy equation is integrated over the computational domain to get:

$$H_i = Q_{kx} - Q_{cx} + Q_{ky} - Q_{cy} + Q_r$$

where Q_{kx} and Q_{ky} are the contributions due to conduction (x, y), Q_{cx} and Q_{cy} those due to convection (x, y) and Q_r the heat needed for the reactions to occur. They can be detailed as follows (see Fig.1 for the integration domain):

$$H_i = \int_0^{X_s}\int_0^{Y_s}\left(\frac{\partial(c_W\varrho_W + c_A\varrho_A + c_C\varrho_C + \varepsilon c_g\varrho_g)(T-T_o)}{\partial t}\right)dydx \tag{11}$$

$$Q_{kx} = \int_0^{Y_s}\left(k_x^*\frac{\partial T}{\partial x}\right)_{x=X_s}dy,\ Q_{ky} = \int_0^{X_s}\left(k_y^*\frac{\partial T}{\partial y}\right)_{y=Y_s}dx \tag{12}$$

$$Q_{cx} = \int_0^{Y_s}(c_g\varrho_g(T-T_0))_{x=X_s}dy,\ Q_{cy} = \int_0^{X_s}(c_g\varrho_g(T-T_0))_{y=Y_s}dx \tag{13}$$

$$Q_r = \int_0^{X_s}\int_0^{Y_s}(r_1\Delta h_1 + r_2\Delta h_2 + r_3\Delta h_3)\,dydx \tag{14}$$

The contributions (12-14) are reported in Fig.6 as functions of time. Q_{ky} is always larger than Q_{kx} and both of them decrease as time increases owing to the temperatures at the surface approaching to the final furnace temperature. Q_r attains its maximum value at the beginning of the degradation process when the resistance to heat transfer is low. Interesting is also the time dependence of the heat convected out by the pyrolysis products. In agreement with the degradation process previously described, Q_{cx} is initially larger than Q_{cy}, but rapidly decays to very low values. On the contrary, Q_{cy} assumes rather large values as long as the solid is undergoing pyrolysis. Thus convective transport of heat along solid grain plays a role of increasing importance for long times when conductive transport values lower. Indeed, the integral forces driving heat transfer interior to the solid are: $Q_{dx} = Q_{kx} - Q_{cx}$ and $Q_{dy} = Q_{ky} - Q_{cy}$. These two contributions reported in Fig. 7 as functions of time, clearly indicate that, beyond certain times, a positive integral contribution to inward heat transfer is established only along the x direction (cross grain). In the same figure, a comparison can be made with the equivalent net integral forces driving heat interior to the solid for the same pyrolysis process simulated in the absence of convective heat transport, that is Q'_{kx} and Q'_{ky}. In this case most of the heat is transferred along grain (y) because of the larger thermal conductivities. As expected, Q'_{kx} and Q'_{ky}, during the transients of the process, are larger than Q_{dx} and Q_{dy}. However, for $t > 90s$, an inversion is observed for the cross grain direction (x) because the absence of convective cooling causes a faster attainment of steady surface temperatures.

The different thermal history of the degrading solid along the x and y directions also exerts some influence on the chemical pathways. Because of the lower activation

energy, reaction (2) (char and gas formation) is favored at low temperatures. As can be observed from Fig. 8, char densities increase with the distance from the exposed surfaces (progressively lower reaction temperatures) and are larger along the solid grain (lower temperatures).

When 90% of the solid has undergone pyrolysis, char represents 4% of the initial weight of the solid. As char and gas productions are linked, it can be inferred that primary gas yield is 7.4%, the remaining amount being tar. Char yield lowers to 3.6% for the case of no convective transport of heat. In this case the conversion time is also shorter (180s against 230s).

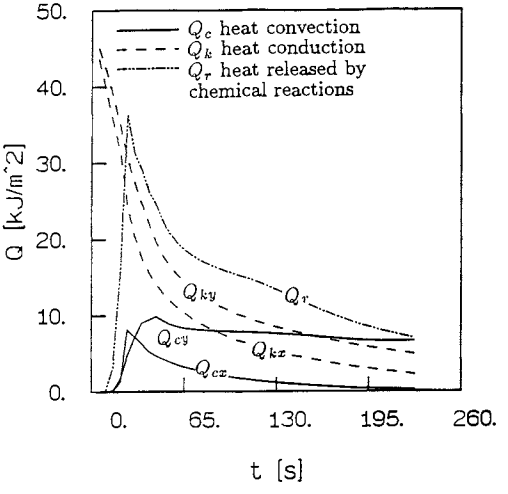

Figure 6 - Q_{kx}, Q_{ky}, Q_{cx} and Q_{cy} as functions of time for $T_f = 900K$.

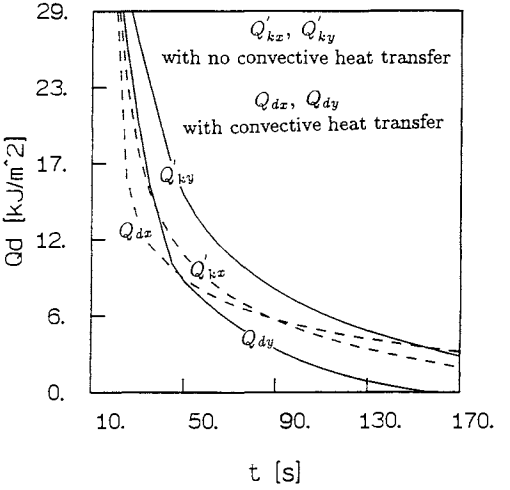

Figure 7 - Q'_{kx}, Q'_{ky}, Q_{dx} and Q_{dy} as functions of time for $T_f = 900K$.

The pyrolysis of the $0.02m \times 0.02m$ wood sample is always controlled by heat transfer, as the furnace temperature is varied. For high furnace temperatures ($> 700K$), the reaction front is very steep and the spatial gradients of main variables are very large. For main lines, the characteristics of the process are similar to those already presented for $T_f = 900K$. For low reactor temperatures ($< 700K$), the thickness of the reaction zone enlarges and, apart from a narrow zone close to the exposed surfaces, the devolatilization process occurs at almost the same time along the whole sample, with much lower spatial gradients. The dynamics of the solid weight loss and its rate are shown in Fig.9 for reactor temperatures from $600K$ to $1000K$. For all cases an initial period of slow weight loss is simulated, this being most noticeable for the lower temperatures. For high furnace temperatures, a sharp rise in the rate of solid devolatilization, due to the degradation of a narrow zone close to the heated surfaces, is followed by a strong decrease, due to the process becoming heat transfer controlled. At low furnace temperatures the rate of weight loss shows a slow increase to significant values which are maintained for a rather long period of time, followed then by a slow decrease.

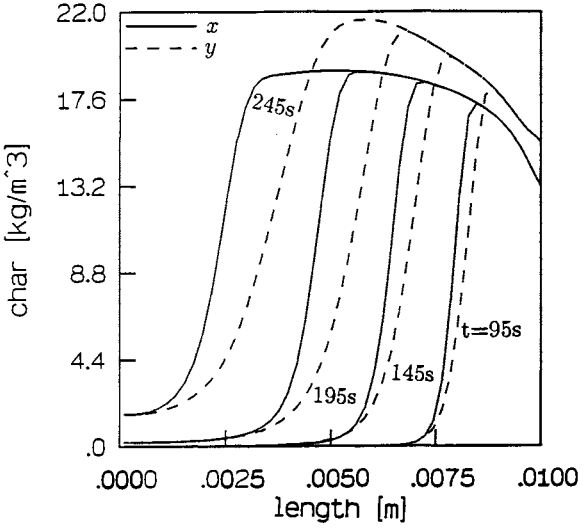

Figure 8 - Char density profiles along the x (solid lines) and y (dashed lines) axes for times reported in the figure and for $T_f = 900K$.

The dependence of the char yield, expressed as % of the initial weight of the solid at conversion conditions of 90%, and conversion time on the furnace temperature is reported in Fig. 10. According to experimental evidence [6,7,11,12], both the char yield and the conversion time decrease as the furnace temperature is increased, with a high rate of variation in the range of temperatures $600K - 800K$. Indeed, even for very high furnace temperatures, apart from the initial transients, the heat transfer from the exposed surface to the cold solid is controlling. Also, primary degradation of a large part of the solid sample occurs at temperatures much lower than those established in

the furnace. Under these conditions, the primary reaction paths are less and less affected by the temperatures of the char layer and both conversion time and char yield tend to a constant value. Finally, it is worth observing that, for the range of furnace temperature here considered, tar is the main product of primary degradation and gas phase flaming combustion is highly favored.

CONCLUSIONS

Two-dimensional, unsteady balance equations for chemical species, energy and momentum have been used to simulate the pyrolysis of a cellulosic material. The large number of parameters and the large uncertainty about values and dependence on conversion conditions make any quatitative comparison between predictions and experimental

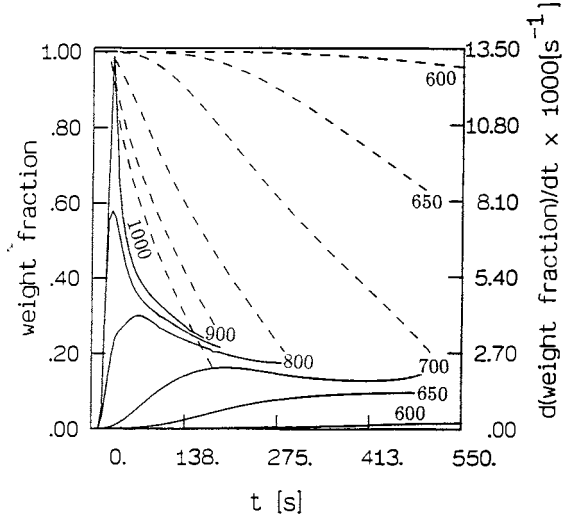

Figure 9 - Weight fraction (dashed lines) and time derivative of the weight fraction (solid lines) as functions of time for several values of the furnace temperature [K].

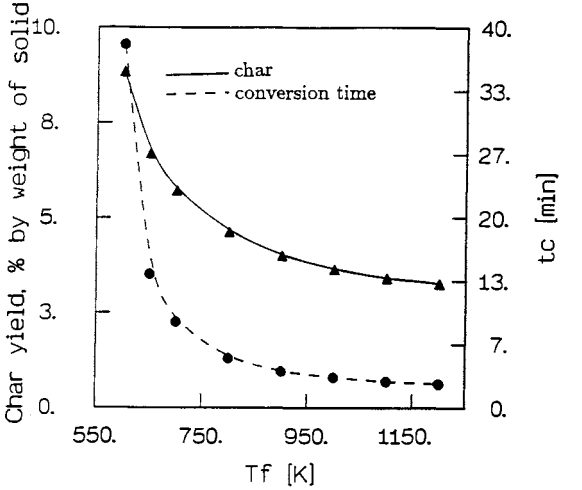

Figure 10 - Char yield, expressed as % of the initial weight when 90% of the solid has been degraded, and conversion time as functions of the furnace temperature.

results difficult. However, a qualitative agreement is obtained and the model predictions have given some information on the physical mechanisms affecting the pyrolysis of large cellulosic samples. The pyrolysis process is heat transfer controlled and presents a wave-like character with the propagation of pressure and reaction fronts from the exposed surface towards the interior of the sample. The rate of advance of these fronts is affected by the grain structure of the solid. Notwithstanding the larger thermal conductivities along solid grain, the larger convective cooling, associated with the larger volatile mass fluxes along this direction, makes the advancement of the degradation fronts slower. The char yield and the conversion time decrease as the furnace temperature is increased, but, given the large size of the sample, the degradation of the solid is always controlled by heat transfer.

Further improvements in the mathematical formulation of cellulosic material pyrolysis should include the description of secondary reactions whose extent is influenced by both the medium thermal conductivities (reaction temperatures) and permeabilities (volatile residence times).

REFERENCES

1) Kanury, M. A., "Thermal decomposition kinetics of wood pyrolysis", Combustion and Flame, 18: 75-83, 1972.

2) Chan, W. R., Kelbon, M., and Krieger, B., "Modelling and experimental verification of physical and chemical processes during pyrolysis of large biomass particle", Fuel, 64: 1505-1513, 1985.

3) Di Blasi, C., "Analysis of convection and secondary reaction effects within porous solid fuels undergoing pyrolysis", Combustion Science and Technology, 90: 315-339, 1993.

4) Di Blasi, C., "Numerical simulation of cellulose pyrolysis", Biomass and Bioenergy, in press, 1994.

5) Di Blasi C., "Modeling and simulation of combustion processes of charring and non-charring solid fuels", Progress in Energy and Combustion Science, 19: 71-104, 1993.

6) Broido, A., and Nelson, M. A., "Char yield on pyrolysis of cellulose", Combustion and Flame, 24: 263-268, 1975.

7) Bradbury, A. G. W., Sakai, Y., and Shafizadeh, F., "A kinetic model for pyrolysis of cellulose", Journal of Applied Polymer Science 23: 3271-3280, 1979.

8) Chan, W. R., Kelbon. M., Krieger-Brockett, B., "Single-particle biomass pyrolysis: correlation of reaction products with process conditions", Ind. Eng. Chem. Res., 27: 2261-2275, 1988.

9) Di Blasi, C., "Smolder spread through thin horizontal fuel layers", Proc. of the Third (Int.) Conference on Advanced Computational Methods in Heat Transfer, in press, 1994.

10) Lee, C. K., Chaiken, R. F., and Singer, J. M., "Charring Pyrolysis of wood in fires by laser simulation", Sixteenth Symposium (Int.) on Combustion, The Combustion Institute, Pittsburgh, pp. 1459-1470, 1976.

11) Hajaligol, M. R., Howard, J. B., Longwell, J. P., and Peters, W. A., "Product Compositions and kinetics for rapid pyrolysis of cellulose", Ind. Eng. Chem. Process Des., Dev., 21: 457-465, 1982.

12) Scott, D. S., Piskorz, J., Bergougnou, M. A., Graham, R., and Overend, R. P., "The role of temperature in the fast pyrolysis of cellulose and wood", Ind. Eng. Chem. Res., 27: 8-15, 1988.